Surface properties of graphene oxide reinforced polyvinyl chloride nanocomposites

Kalim Deshmukh · S. M. Khatake · Girish M. Joshi

Abstract Graphene derivatives are intensively used as high performance nano fillers for the fabrication of polymer nanocomposites. The challenge is to achieve significant improvement in interfacial adhesion between polymer matrix and reinforcing filler. In the present work, we report the preparation of polyvinyl chloride (PVC) /Graphene Oxide (GO) composite by the colloidal blending method. PVC/GO composite films were further studied using fourier transform infrared spectroscopy (FTIR), scanning electron microscopy (SEM), transmission electron microscopy (TEM), atomic force microscopy (AFM) and polarized optical microscopy (POM). The effect of GO loading on wettability of PVC/GO composites films were studied by measuring contact angle of composites films. Optical microscopy reveals that GO have been dispersed homogeneously throughout the PVC matrix. From morphological studies, a network of a denser stacking and randomly aggregate structure having rough surface was observed as a function of GO loading. The values of contact angle decrease with respect to GO loading for all the liquids used. The solid surface energy (SE) of composite films was estimated using contact angle measurements. The surface energies were measured and compared using Fowke's and Good-Grifalco methods with respect to four different liquids having a wider range of surface tensions ($44 \leq lv \leq 72.8$ mJ/m^2). The composite film surfaces were tuned by controlling incorporation of GO in order to optimize the surface roughness.

Keywords Graphene · PVC · Colloidal blending · Surface roughness · Surface energy

K. Deshmukh · S. M. Khatake · G. M. Joshi (✉)
Polymer Nanocomposite Laboratory, Material Physics Division,
School of Advanced Sciences, VIT University,
Vellore 632014, TN, India
e-mail: varadgm@gmail.com

Introduction

Ever since its discovery, graphene based polymer nanocomposites have been the subject of intensive investigations among researchers across the globe. Graphene has been used as viable and inexpensive filler for polymer nanocomposite due to its ability to be dispersed in various polymer matrices and its extraordinary chemical and physical properties such as high specific surface area [1] high charge carrier mobility [2], flexibility and high young's modulus [3, 4] and high thermal conductivity [5]. At extremely small loadings, a significant improvement in the physical properties of host polymers can be achieved if incorporation of graphene is appropriate. Graphene consists of one atom thick planar sheet comprising of SP^2 bonded carbon structure with exceptionally high crystal and electronic properties [6]. It can be rolled into zero dimensional (0D) fullerenes, one dimensional (1D) nanotubes and can be staked to form three dimensional (3D) graphite [7]. Graphene is a novel material which has been used in many areas of research due to its remarkable physicochemical properties. Graphene has unusual electronic properties such as the anomalous quantum Hall effect which is due to special electronic structure of graphene [8] and high carrier mobility at relatively high charge carrier concentration at room temperature [9]. To confirm the superiority of graphene to traditional materials, many interesting properties such as electrical [10], thermal [1] and mechanical [3] have been reported. The impact of graphene as a nanofiller in various polymeric systems such as, polystyrene (PS), polycarbonate (PC), polyurethane (PU), polyethylenetrephthalate (PET), polyaniline (PANI), polyvinylidenefluoride (PVDF), Nafion, etc. has been studied with an interest to develop high performance graphene based nanocomposites for wide range of applications [11].

Recently, graphene oxide (GO) has attracted substantial interest as a promising precursor for preparing graphene and graphene based polymer nanocomposites. The focus is primarily

on the preparation of polymer nanocomposites using GO or its allotropes as a filler with an emphasis on enhancement in the properties of composites for various applications [12]. Like graphene, GO is essentially one-atom thick but can be as wide as tens of micrometers, resulting in a unique type of material building block, characterized by two very different length scales [13]. GO sheets are highly oxygenated having hydroxyl and epoxy functional groups on their basal plane, in addition to carbonyl and carboxyl groups located at the sheet edges [14]. These functional groups provide reactive sites for various surface modifications to develop functionalized GO and its allotropes [15]. The presence of these functional groups makes GO sheets strongly hydrophilic which allows GO to readily disperse in water to form stable colloids. Owing to their hydrophilic nature, GO sheets can only be dispersed in aqueous media which is incompatible with organic polymers [16]. GO is also a center of attraction amongst many researchers all over the world because it has many exceptional properties which may lead to technological applications in many fields, such as energy storage, composite materials, chemical sensors and optical and electronic devices [15]. To take the advantage of the structure and physical properties of the graphite derived carbon materials such as graphene, GO, chemically reduced GO (CRGO) or thermally reduced GO (TRGO) or functionalized graphene sheets (FGS), there are several key factors to be considered in the fabrication of polymer nanocomposites: degree of dispersion, orientation and interfacial adhesion [14, 17, 18].

Wetting is a fundamental interfacial phenomenon in which one fluid phase is displaced completely or partially by another fluid phase from the surface of a solid or liquid. Contact angle is a measure of the wettability and surface roughening of polymer surfaces. If the contact angle is much smaller than the liquid is said to wet the solid. Therefore, the aim of the present work is to fabricate PVC nanocomposites with GO by colloidal blending method and to study their surface properties. To evaluate wettability and surface roughness of composite films we employed contact angle goniometry and AFM techniques. We chose PVC as a host material because it is one of the most important commercial polymers with vast applications in several areas of the material industry, such as flexible or rigid plastic molds, pipes, electric cables, fibers, films and laminates [19]. It is one of the most important and widely used thermoplastics in the construction and automotive industries due to its many valuable properties like low cost, good processability, chemical stability, biocompatibility and low flammability. The combination of the unique properties of GO and good processability of polymer would open up possibilities for making advanced polymer nanocomposites with new physicochemical properties. In order to have efficient reinforcement in polymer composites, it is important to have molecular level dispersion in the polymer matrix [20]. We readily dispersed both GO and PVC in Tetrahydrofuran (THF) to achieve molecular level colloidal dispersion.

Experimental

Materials

PVC granules used in this study was kindly supplied by Technovinyl Polymers Ltd., Mumbai, India, with specific gravity of 1.38 (±0.03), tensile strength of 22.8 MPa, Elongation at break 200 (%), volume resistivity of 8×10^{14} Ohm/cm and processing temperature in the range of 150° to 185 °C. Graphite was supplied by Carbotech Engineers, Jaipur, Rajasthan, India. THF, extra pure AR grade was purchased from Sisco Research Laboratory (SRL) Chemicals, Mumbai, India. Glycerol (G), Ethylene Glycol (EG) and Dimethylsulfoxide (DMSO) were obtained from S. D. Fine Chemicals, Ltd; Mumbai, India. Ultrapure Milli-Q water was used throughout the study. PVC and all the chemicals were used as received without further modification.

Synthesis of graphene oxide (GO)

Graphite was subjected to an oxidative treatment with potassium permanganate ($KMnO_4$) in concentrated sulphuric acid (H_2SO_4). GO was produced from natural graphite according to the modified Hummers method [21]. Graphite powder (3 gm) and $NaNO_3$ (3 gm) were charged into a 1000 ml round bottom flask. Concentrated H_2SO_4 (150 ml) was then added to the flask and mixed well. The mixture was kept in an ice bath for 4 h with stirring at temperature 5 °C. Afterwards, $KMnO_4$ (9 gm) was gradually added with constant stirring and the rate of addition was controlled carefully to avoid sudden increase in temperature. The ice bath was then removed and the mixture temperature was maintained at 40 °C and stirred for 2 h until the color become brown. Subsequently, 150 ml deionized water was added for dilution. Finally, the mixture was stirred at 98 °C for about 1 h until the color changed from brown to yellow. Furthermore, the mixture was stirred for another 10 min. and then diluted by adding 700 ml deionized water. After 1 h 30 ml of H_2O_2 (30 wt%) solution was
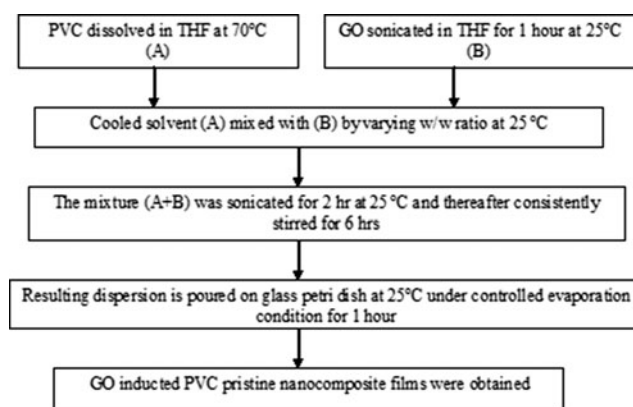
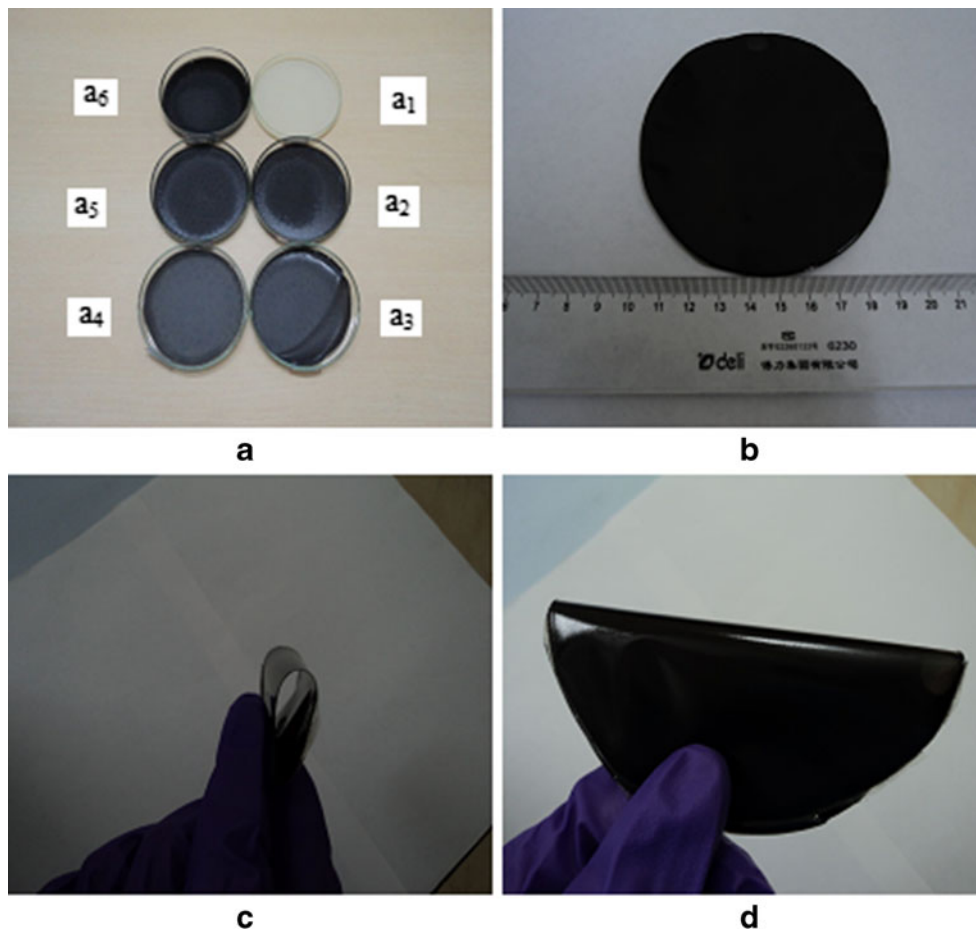
Fig. 1 Protocol for synthesis of PVC/GO pristine composites
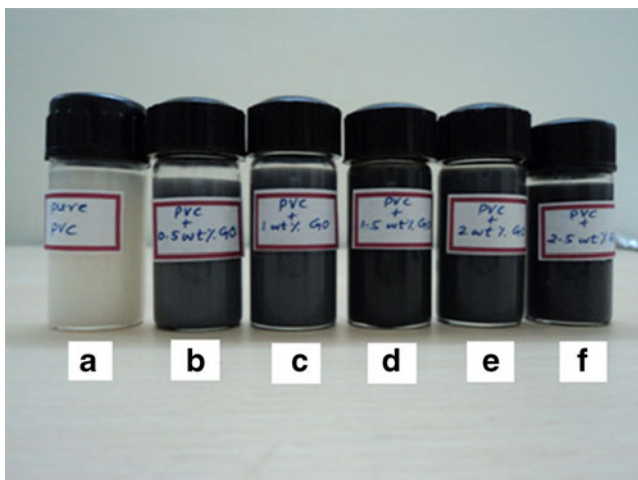
Fig. 2 Photographs showing dispersion behavior of PVC/GO in THF after sonication (**a**) Pure PVC solution (**b**) 0.5 (**c**) 1 (**d**) 1.5 (**e**) 2 (**f**) 2.5 wt% GO loading
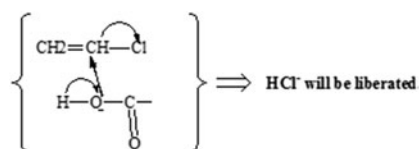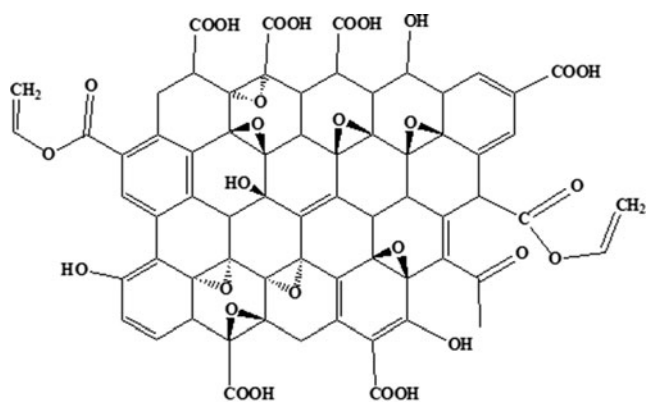
added to the mixture to reduce residual $KMnO_4$. Finally, the solution was then filtered and washed several times with deionized water until pH became 7 and dried at 60 °C for 12 h to obtain GO powder.

Preparation of PVC/GO composite films

Colloidal blending method was used to fabricate PVC/GO composite films. A protocol of synthesis is given in Fig. 1. A known quantity of PVC was first dissolved in THF at 70 °C. GO powder was separately dispersed in THF and sonicated for 30 min. at room temperature before mixing it with PVC solution. The mixture was further sonicated for 1 hour. The resulting homogeneous dispersion was cast in glass petri dish and kept in an oven at 60 °C for slow evaporation of the solvent to get pristine PVC/GO composite films. The cast films were peeled off from the glass plate and used for further study. The % loading of GO in PVC/GO composite was varied from 0.5 wt% to 2.5 wt%. Figure 2 shows the photographs of different compositions of PVC/GO composite solutions in THF indicating formation of homogenous dispersion. The photographs of different compositions of cast PVC/GO composite films are shown in Fig. 3. A schematic representation of the bonding interaction between PVC and GO is shown in Scheme 1, where it is shown that chemical bonding between PVC and GO takes place due to the formation of an ester linkage. Previous reports demonstrate that

Fig. 3 Photographs of PVC/GO composite films prepared by colloidal blending method (**a**) PVC/GO composite film cast on glass plates (a_1) virgin PVC film (a_2) PVC/0.5% GO (a_3) PVC/1% GO (a_4) PVC/1.5% GO (a_5) PVC/2% GO (a_6) PVC/2.5% GO (**b**) PVC/GO composite film indicating uniform dispersion of GO within PVC matrix (**c**, **d**) composite films are bent to demonstrate its flexibility

Scheme 1 Schematic representation of the bonding interaction between PVC and GO

the oxygen containing group of GO can interact with PVC by halogen bonding [22, 23] and serve as an active sites to anchor functional groups making GO compatible with PVC [24].

Characterization of composite films

Surface morphology and structure of PVC/GO composite film was examined by transmission electron microscopy (TEM) using a FEI Technia G20 instrument operated at 200 kV and scanning electron microscope (SEM, JEOL JSM-6360A, Germany with voltage range 0.5 V to 30 kV, magnification 300,000X).
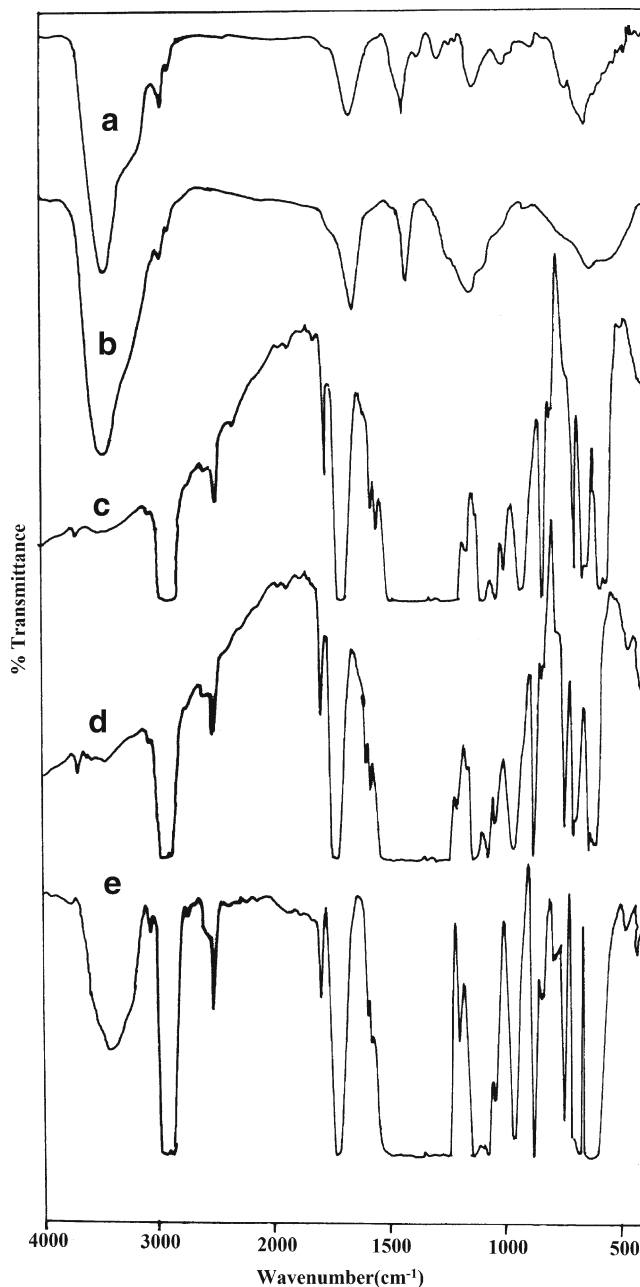
FTIR spectroscopy of PVC/GO composite film was carried out with Fourier Transform Infrared Spectrophotometer (Shimazdu, IRAffinity-1, Japan) in the wave number range 400–3500 cm^{-1} in a transmittance mode.

Optical microscopy of GO reinforced PVC composites was investigated by Carl Zeiss AX10 vision LE optical microscope at 25 °C.

The morphology of as prepared samples was determined by typical tapping mode atomic force microscopy (NanoSurf Easy Scan2, Switzerland) operating in the air. For AFM studies samples were prepared by sticking a small piece of composite film on a glass slide. All images were taken at 25 °C with scanning raster rate of 1 Hz.

Contact angle measurements were carried out by using the sessile drop method [25, 26]. The contact angle of water (W), glycerol (G), dimethylsuphoxide (DMSO), and ethylene glycol (E.G), on the surfaces of PVC/GO composite films, were measured using a contact angle meter. The contact angle is usually measured by the

tangent at the three phase interface (solid-liquid-vapor) [27]. The liquid drop (~2–3 μl) was placed on to the surface of PVC/GO composite film with the help of micro syringe. The image of liquid is directly projected on the screen. The screen has two calibrated axes mutually perpendicular to each other, which can be rotated. The surface energy (SE) was calculated from contact angle measurements using Fowkes [28] and Good and Girifalco model [29]. The error involved in contact angle measurement was around ±1.5.

Fig. 4 FTIR spectra of PVC/GO composite film (**a**) Pure PVC (**b**) 0.5 (**c**) 1 (**d**) 1.5 (**e**) 2 wt% GO loading

Table 1 Peak assignment for PVC, GO and PVC/GO composites

Wavenumbers (cm^{-1})	Peak assignments
2924	C-H Stretching
1265	C-H Rocking
960	Trans CH Wagging
833	C-ClStretching
601	Cis CH Wagging
1074	C-C Stretching
1126	C-C Stretching, CH$_2$ Wagging
1199	HC-Cl Bending, CH$_2$ Wagging
1442	CH$_2$ Wagging

Results and discussion

FTIR spectroscopy of PVC/GO composite films

FTIR is a very important tool for investigating the structures of polymer composites. Due to variation in different compositions and interaction between the components of the composites, one can expect change in FTIR spectra. The FTIR spectra of PVC and PVC/GO composite films are shown in Fig. 4. The FTIR peak assignments are given in Table 1. The characteristic band of PVC was observed at 2924 cm^{-1} which can be assigned to C-H stretching vibrations. The bands at 1265 cm^{-1} and 960 cm^{-1} are assigned to CH-rocking and *trans* CH wagging vibrations respectively. Also the band at 833 cm^{-1} was observed which corresponds to stretching of C-Cl band and the band at 616 cm^{-1} is assigned to *cis* CH wagging vibrations. The bands at 1074 cm^{-1} and 1442 cm^{-1} can be attributed to C-

C stretching and CH$_2$ wagging respectively. The absorption peaks of PVC were observed at 1717, 1244 and 1089 cm^{-1} and the vibrational bands were observed at 1332 and 682 cm^{-1}. The FTIR spectra of GO shows peaks at 1725 cm^{-1} and 1220 cm^{-1} which are corresponding to C=O and C-O stretching vibration respectively. Besides, the carboxylic group has the peaks of symmetric and asymmetric stretching vibration at 1600 and 1380 cm^{-1} respectively. The bands at 3419 cm^{-1} is corresponds to OH- stretching vibration [30]. FTIR spectra of PVC/GO composite films show an increase in the intensity of the peak at 2924 cm^{-1} which is attributed to C-H stretching vibrations of PVC. Also peak of the OH-stretching vibration in GO at 3419 cm^{-1} becomes broader at higher loading of GO (1.5 wt%) in PVC/GO composite films.

Optical microscopy of PVC/GO composite films

One of the most important requirements to effectively enhance the properties of polymer matrix is to achieve homogeneous dispersion of filler in composite. The objective of an optical microscopy is to understand the dispersion of GO in polymer matrix. Optical microscopy also helps in understanding the reinforcement of fillers in a polymer matrix and/or the aggregation /clustering of fillers [31]. Figure 5 shows optical microscopy images of PVC/GO composites. It can be seen that GO have been dispersed homogeneously throughout the PVC matrix. This can be observed thoroughly in the micrographs, even at very low concentrations (0.5 wt%). However at higher loading of GO as shown in Fig. 5(g), some aggregation take place. Therefore one has to optimize the inherent properties of nanofiller in dispersion and nanoscale morphology in polymer

Fig. 5 Optical microscopy images of PVC/GO composites (**a**, **b**) Pure PVC (**c**, **d**) 0.5 (**e**, **f**) 1 (**g**, **h**) 1.5 (**i**, **j**) 2 (**k**, **l**) 2.5 wt% GO with X100 and 200 μm resolution
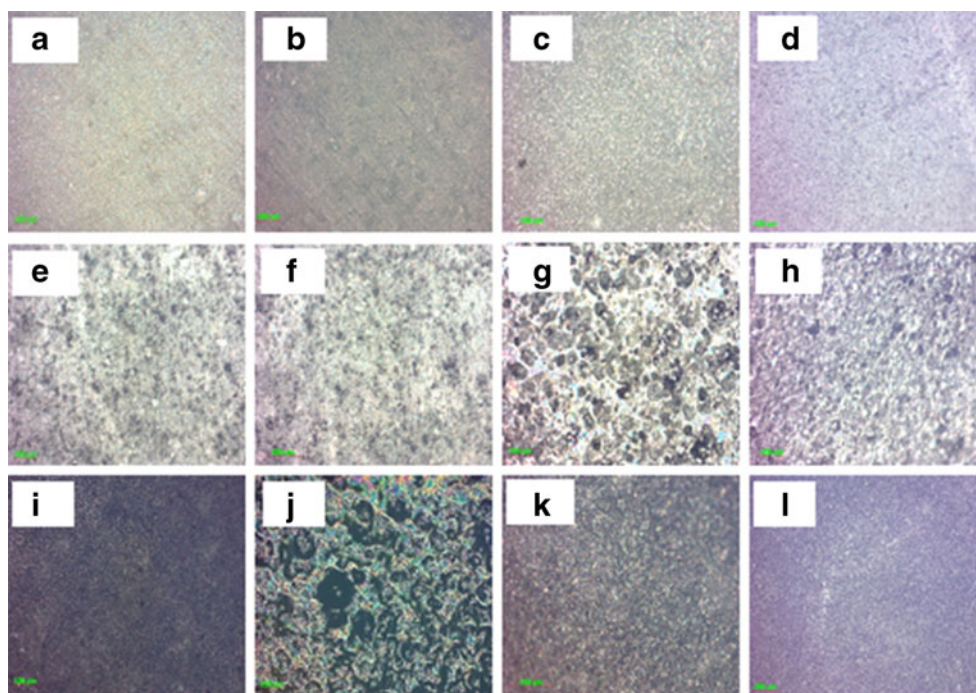
Fig. 6 AFM topographic images of PVC/GO composites (**a**) Pure PVC (**b**) 0.5 (**c**) 1 (**d**) 1.5 (**e**) 2 (**f**) 2.5 wt% GO loading X 25 μm resolution
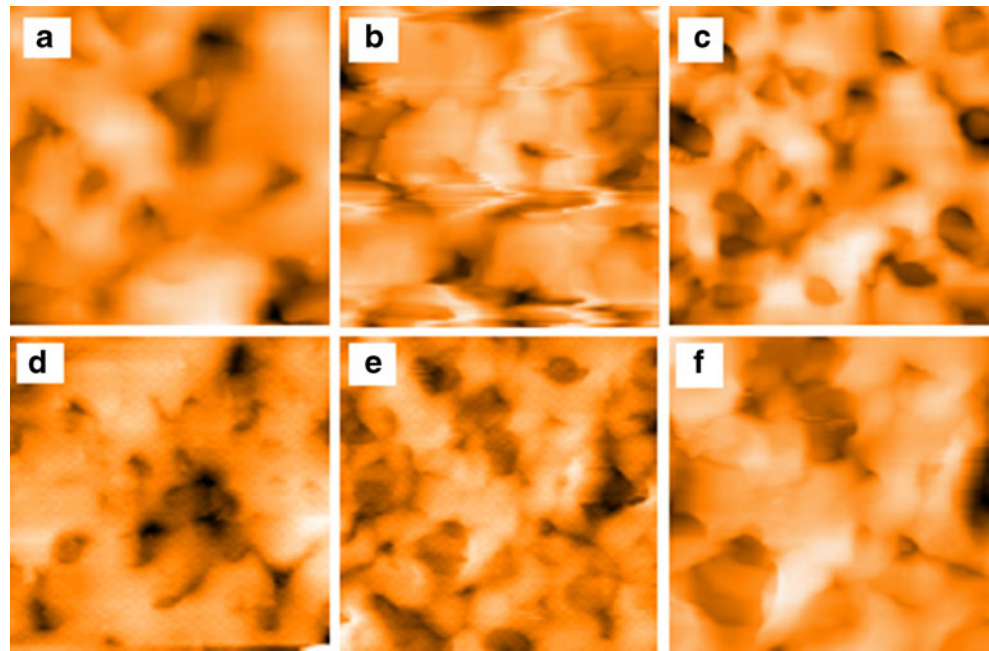

matrix for effective reinforcement of nanofiller into polymer matrix.

Surface morphology and roughness of PVC/GO composite films

The degree of exfoliation after the dispersion of GO in a solvent can be characterized by AFM technique, which is the most direct method. PVC and PVC/GO composite films were characterized by AFM with a tapping mode and the morphology images are depicted in Fig. 6. It was observed that GO as filler has a significant effect over the surface morphology of composite films. The images reflect homogeneous dispersion of GO in PVC without any wrinkles on the surface of the film. The AFM image of the pristine PVC illustrates a very smooth surface with some stripes. For 0.5 wt% GO with PVC softens the surface with average roughness 0.04 ± 0.02 nm. Increases in surface roughness above 1 wt% loaded GO show roughness 800 ± 0.04 nm and the higher value loading increase the surface roughness [20, 32]. Hence the surface tuning is possible by controlling the GO loading and by preparing homogeneous dispersion of PVC/GO in the appropriate solvent for successful preparation of composite film. Figures 7 and 8 shows 3D AFM images and a trend of surface roughness vs. GO loading. Surface roughness of the PVC/GO composite films drastically increase upon

Fig. 7 AFM 3D images of PVC/GO composite film (**a**) Pure PVC (**b**) 0.5 (**c**) 1 (**d**) 1.5 (**e**) 2 (**f**) 2.5 wt% GO loading
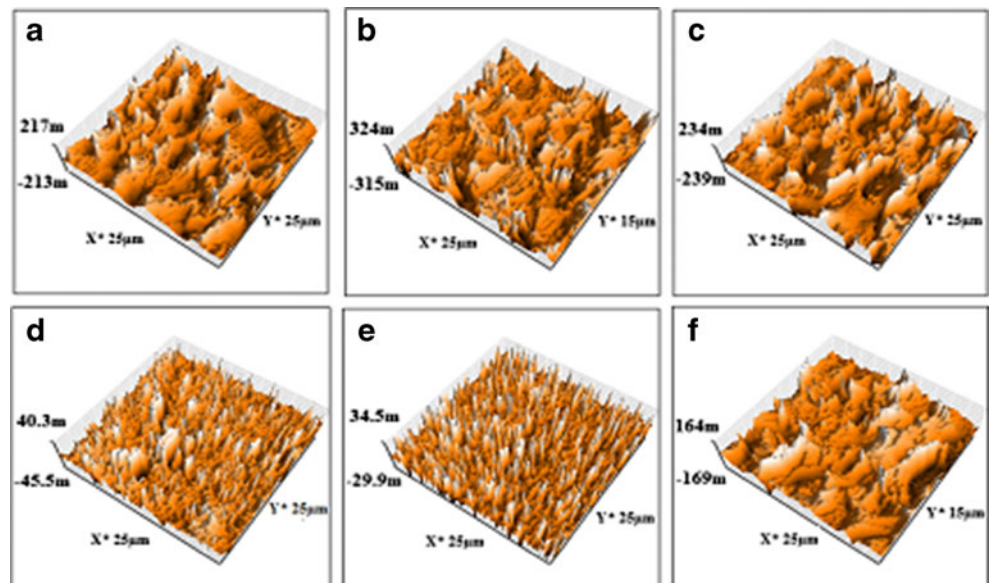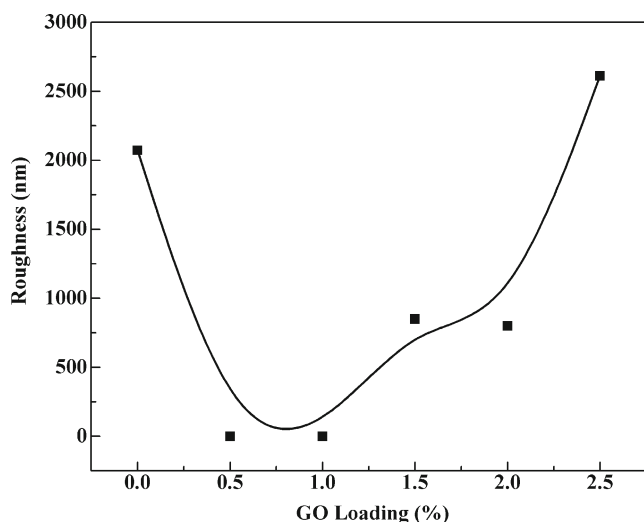
Fig. 8 Variation in surface roughness with respect to GO loading

addition of the GO in PVC matrix compared to the neat PVC, probably because of the fine dispersion of GO throughout the PVC matrix.

Morphology and microstructure of PVC/GO composites

The degree of GO exfoliation in the PVC / GO composite was identified by TEM as shown in Fig. 9. It was observed that GO was well dispersed in THF by ultrasonic treatment. The homogeneous dispersion of filler in composite is one of the most important requirements to effectively enhance the matrix properties. TEM images reveal that GO was uniformly distributed in PVC matrix and there are no large agglomerates observed. Scanning electron microscopy technique is a bottom up approach to yield molecular level dispersion of graphene oxide in polymer matrix. Figure 10(a-f) shows SEM micrographs of PVC/GO composite films. It was observed that increasing GO loading results in significant change in the surface morphology of PVC/GO composite films. SEM micrograph of PVC/GO composite film shows that the majority of GO has been uniformly dispersed
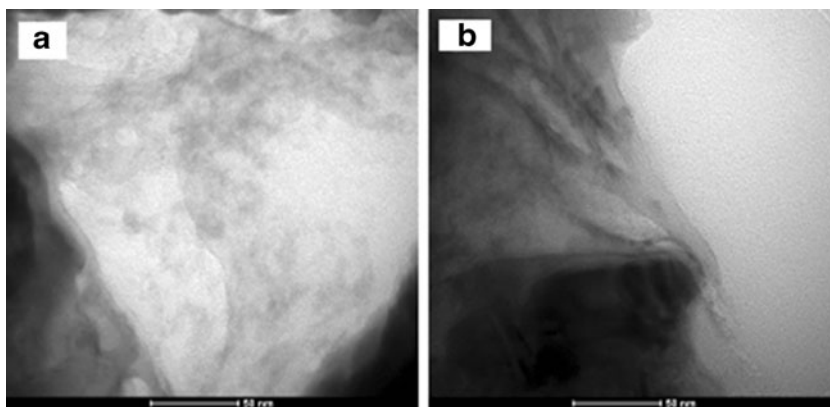
throughout the polymer matrix with low degree of agglomeration. In other words, a network of a denser stacking and randomly aggregate structure having rough surface was observed. This observation can be correlated to AFM results (Fig. 8) where it is evident that the surface roughness increases with respect to increase in GO loading. Also, it is difficult to distinguish the individual phases of GO and PVC in PVC/GO composites films because polymers grow in the pores and galleries of GO [33]. Hence SEM analysis reveals that GO and PVC formed a uniform composite with PVC filled between GO nanosheets resulting in macro porous structure. A better dispersion of PVC/GO composites may contribute in enhancing the electrical properties of composites. With this interest, studies on electrical properties of PVC/GO composite films are already carried out and the results are communicated elsewhere.

Contact angle study of PVC/GO composite films

Contact angle measurement has been used for many years to assess surface wettability and roughness. It gives a better understanding of material compatibility. The wettability is crucial in polymer composite prepared with reinforced nanofillers. In the present work we have used sessile drop method to calculate contact angle. The contact angles measured for probe liquids on solids of interest are used to calculate surface free energies. In practice, the measured contact angle may not fully satisfy the assumptions implicit in the Young's equation. Contact angle measurement is capable of yielding the interfacial properties of the precise, smooth and homogeneous surface of solids [34]. In this study, we observed decreased in the contact angle values of PVC/GO composite film with respect to four different liquids as shown in Fig. 11. For SE measurement the proper choice of a liquid is very important. If $\gamma_{lv} \leq \gamma_{sv}$, the solid will get wet completely; therefore such liquids cannot be used to find the contact angle because the liquid drop becomes flat immediately. Hence SE can also not be measured. Generally, it is advised that we should start contact angle measurement

Fig. 9 TEM images of PVC/GO composite film with 2.5 wt% GO (**a**) and (**b**)

**Fig. 10** SEM micrographs of (**a**) PVC film (**b**) 0.5 (**c**) 1 (**d**) 1.5 (**e**) 2 (**f**) 2.5 wt% GO loading
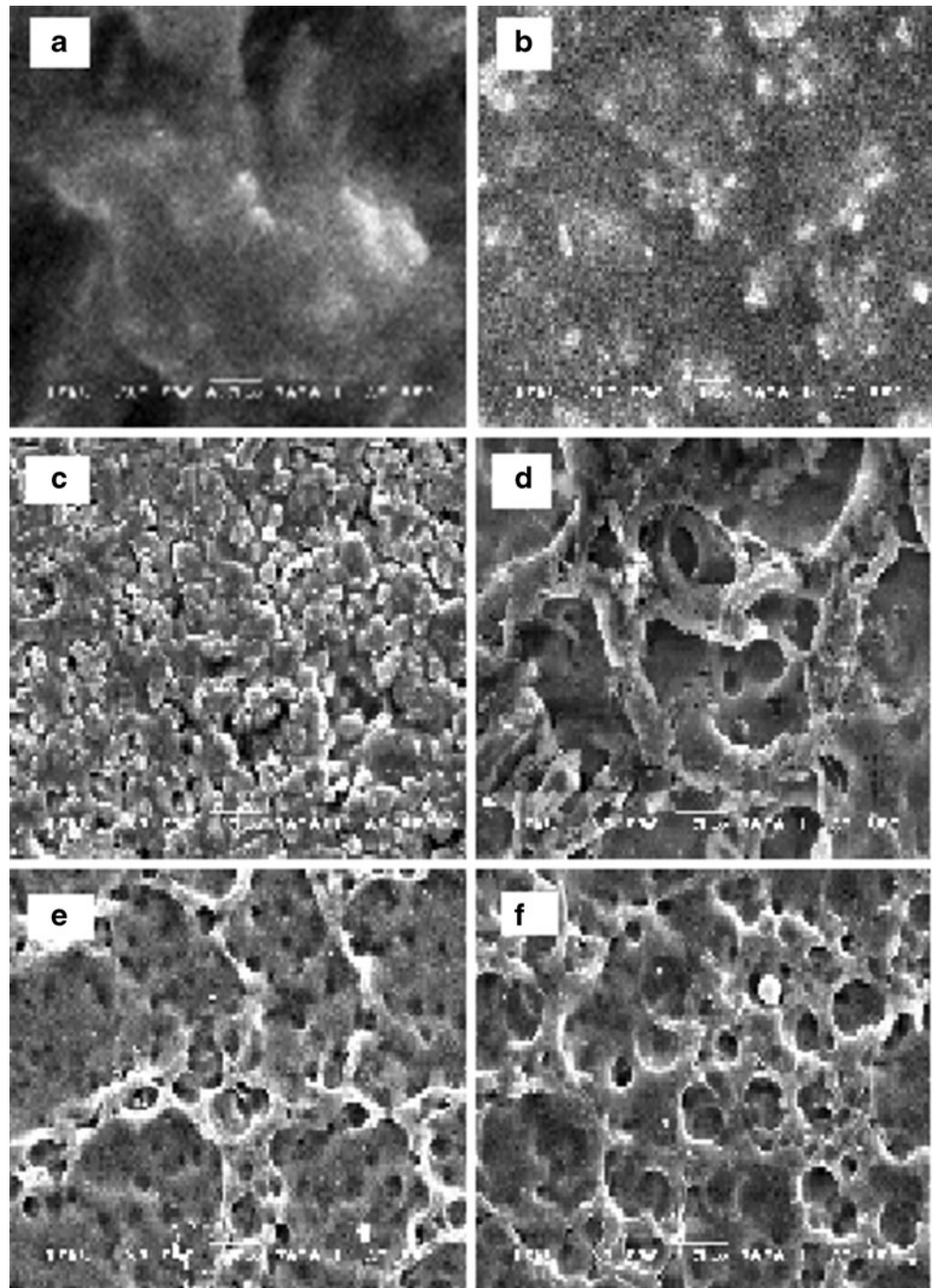
with high surface tension liquid (e.g., water, 72.8 mJ/m^2) as there is a large % error involved in the contact angle measurement. The values of γ_{lv} cosθ increase as γ_{lv} decreases, reaching a global maximum [35]. Thus the surface tensions of the test liquids should be higher than that of the solid surface tension, by the appropriate choice of the liquids. Another possible effect of $\gamma_{lv} < \gamma_{sv}$ is liquid adsorption, which could cause γ_{sv} to be different from liquid to liquid. Therefore, the test liquids used in this study were selected to fulfill the condition $\gamma_{lv} > \gamma_{sv}$ [35].

Evaluation of surface energy by Fowkes method

A set of four different liquids of known polar and disperse components was used to calculate the surface free energy of PVC/GO composite films. The more number of solvents imposed to obtain the average accuracy. Table 2 shows the surface tension for various liquids used in this study. The surface energy (γ_s) can be determined by using following Young's equation [26].

$$\gamma_{lv\cos\theta} = \gamma_{sv} - \gamma_{sl} \tag{1}$$
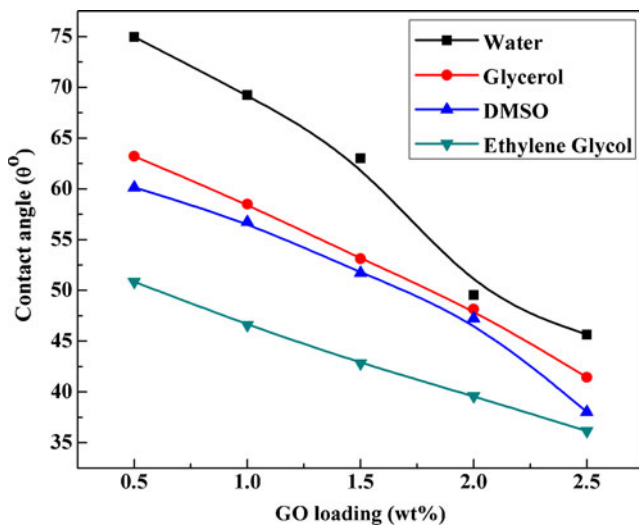
Fig. 11 Contact angle values of PVC/GO composite films with respect to different liquids

Fig. 12 Surface energy calculated using Fowkes and Good-Girifalco method

Where γ_{lv} is the surface tension of a liquid, γ_{sv} is the surface tension of a solid, γ_{sl} is solid-liquid interfacial tension and θ is contact angle.

By using Fowkes approximation [30, 36] we can get the following equation to calculate the surface free energy.

$$\left[\frac{1+\cos\theta}{2}\right] \times \left[\frac{\gamma_l}{\sqrt{\gamma_l^d}}\right] = \sqrt{\gamma_s^p} \times \sqrt{\frac{\gamma_l^p}{\gamma_l^d}} + \sqrt{\gamma_s d} \qquad (2)$$
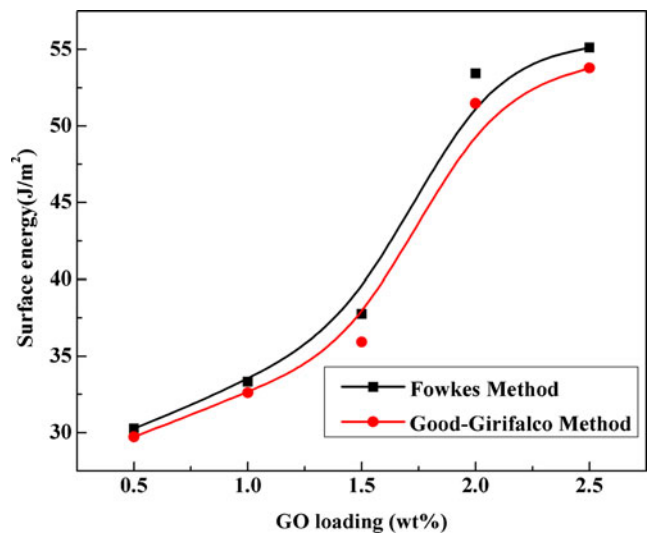
The equation of straight line expressed as Y(LHS) = mX(RHS) (3)

Where value of LHS can be obtained by calculating Y for the liquid used. From Table 2 the values of γ_l and $\gamma_l d$ can be calculated. Similarly, by using polar and disperse components of liquid used, RHS can also be calculated. Fowkes [28, 37] assumed that the surface free energy of a solid and liquid could be considered as a sum of independent components resulting from different intermolecular interactions. Thus,

$$\gamma = \gamma^p + \gamma^d \qquad (4)$$

Where γ^p is a polar component due to dipole-dipole interactions and γ^d is dispersed component. The dispersion component of solid surface energy is correlated to London interactions arising from electron dipole fluctuations. Fowkes method is convenient when applied to non polar polymers. However, this condition is applicable on the basis of independence and the sum of polar dispersed and components.

Evaluation of surface energy by Good and Girifalco method

In 1950 Good et al. formulated a theory of interfacial tension using microscopic consideration. They tried to relate the

Table 2 Surface tension for various liquids used in this study at 20 °C in mJ/m^2

Liquids	Surface tensions (γ_{lv})
Water	72.8
Glycerol	64
Ethylene glycol	48
Dimethyl sulfoxide	44
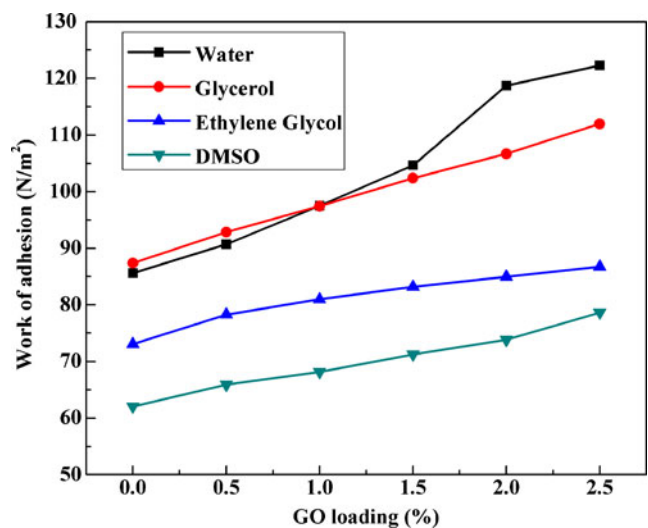
Fig. 13 Work of adhesion as a function of GO loading in PVC/GO composites

interfacial tension between two phases to the geometric mean of the surface tension of each phase. The equation is therefore known as Good-Girifalco equation as given below.

$$\gamma_{12} = \gamma_1 + \gamma_2 - 2\Phi(\gamma_1\gamma_2)^{1/2} \tag{5}$$

Where Φ is the interaction parameter and a characteristics of a given system. When the cohesive and adhesive forces are of the same kind then the interaction parameter become very close to unity. In this case the interaction parameter is given by:

$$\Phi = 4(V_1V_2)^{1/3} / \left(V_1^{1/3} + V_2^{1/3}\right)^2 \tag{6}$$

Where 'V' is molar volumes. When Eq. (2) is substituted in the Young's Eq. (1) we get the following relationship

$$\gamma_s = [\gamma_l(1 + \cos\theta) + \pi_e]^2 / 4\Phi^2 \gamma_l \tag{7}$$

Or neglecting spreading pressure

$$\gamma_s = \gamma_l(1 + \cos\theta)^2 / 4\Phi^2 \tag{8}$$

The Good and Girifalco theory explains the real meaning of Zisman's critical surface tension and its relationship with true solid surface tension [35, 38]. By substituting the definition of critical surface tension in Eq. (7) and expanding in a power series we get.

$$\gamma_C = \Phi^2\gamma_s - \pi_e \tag{9}$$

Where the second subscript of the critical surface tension indicates its dependence on interacting parameters.

Combining Eqs. (8) and (9).

$$\gamma_C = (1/4)(1 + \cos\theta)^2\gamma_l \tag{10}$$

By simply measuring the equilibrium contact angle of single liquid of known surface tension, the surface tension of a given solid can be obtained using Eq. 10. But it will strongly depend up on the liquid because it uses single probe liquid. In this study, we observed slight variation in the surface energy values obtained using Fowkes and Good-Girifalco method as shown in Fig. 12. However, both methods show similar trends of surface energy.

Work of adhesion

The contact angle data can be used to evaluate the work of adhesion. Adhesion and wettability are two related properties. In order to have good adhesion, the adhesive must wet the substrate of the two materials adequately. The equilibrium contact angle for a liquid drop on an ideally smooth, homogeneous and non deformable surface is related to the various interfacial tensions by Young's equation shown in Eq. (1).

Moreover, the work of adhesion W_{adh} of a liquid on a solid surface was calculated by the following equation [39, 40].

$$W_{adh} = \gamma_{lv(1 + \cos\theta)} \tag{11}$$

Work of adhesion was calculated from contact angle with reference to all four liquids studies and depicted in Fig. 13. It clearly shows that there is a pronounced rise in the work of adhesion as the wt% of GO increases.

Conclusions

Flexible PVC/GO composite films were successfully prepared by colloidal blending. Homogeneous dispersion of PVC with GO was achieved by ultrasonic treatment. TEM, SEM, FTIR, AFM and optical microscopy were used to characterize the composite films. FTIR spectroscopy revealed structural changes with respect to different wt% of GO loading. AFM topographic and three dimensional images reveal the variation in surface morphology and roughness as a function of GO loading. SEM analysis reveals that the majority of GO has been uniformly dispersed throughout the polymer matrix with low degree of agglomeration. Contact angle values are inversely proportional to GO loading whereas surface energy and work of adhesion is directly proportional to GO loading. The accuracy of surface energy measurement was achieved by Fowkes method as compare to Good-Girifalco method. Thus, we believe that, this investigation has lot of scope to tailor the optimized surface properties of these synthetic composites.

References

1. Balandin AA, Ghosh S, Bao W, Calizo I, Teweldebran D, Lau CN (2008) Nano Let 8:902–905
2. Bolotin KI, Sikes KJ, Klima M, Fudenberg G, Hone J, Kim P, Stormer HL (2008) Solid State Commun 146:351–355
3. Lee C, Wei X, Kysar JW, Hone J (2008) Science 321:385–388
4. Dumitrica T, Kodambaka S, Jun S (2012) J Nanophotonics 6:1–22
5. Ghosh S, Bao WZ, Nika DL, Subrina S, Pokatilov EP, Lau CN, Balandin AA (2010) Nat Mater 9:555–558
6. Vadukumpully S, Paul J, Valiyaveettil S (2009) Carbon 47:3288–3294
7. Geim AK, Novoselov KS (2007) Nat Mater 6:183–191
8. Novoselov KS, Jiang Z, Zhang Y, Morozov SV, Stormer HL, Zeitler U, Maan JC, Bobinger GS, Kim P, Geim AK (2007) Science 315:1379–1379
9. Nevoselov KS, Geim AK, Morozov SV, Jiang D, Zhang Y, Dubonos SV, Grigorieva IV, Firsov AA (2004) Science 306:666–669

10. Orlita M, Faugeras C, Plochocka P, Neugebauer P, Martinez G, Maude DK, Barra AL, Sprinkle M, Berger C, Heer WAD, Potemski M (2008) Phys Rev Lett 101:267601–267604

11. Kuilla T, Bhadra S, Yao D, Kim NH, Bose S, Lee JH (2010) Prog Polym Sci 35:1350–1375

12. Potts JR, Dreyer DR, Bielawski CW, Ruoff RS (2011) Polymer 52:5–25

13. Kim F, Cote LJ, Huang J (2010) Adv Mater 22:1954–1958

14. Bian J, Xiao M, Wang S, Wang XLY, Meng Y (2009) Chem Eng J 147:287–296

15. Singh V, Joung D, Zhai L, Das S, Khondaker SI, Seal S (2011) Prog Polym Sci 56:1178–1271

16. Hirata M, Gotou T, Ohba M (2005) Carbon 43:503–510

17. Kim H, Abdala AA, Macosko CW (2010) Macromolecules 43:6515–6530

18. Wan C, Chen B (2012) J Mater Chem 22:3637–3646

19. Rusen E, Marculescu B, Butac L, Preda N, Mihut L (2008) Fullerenes, Nanotubes and Nanostructures 16:178–185

20. Vadukumpully S, Paul J, Mahanta N, Valiyaveettil S (2011) Carbon 49:198–205

21. Hummers WSJ, Offman RE (1958) J Am Chem Soc 80:1339–1339

22. Metrangolo P, Meyer F, Pilati T, Resnati G (2008) Terraneo G Angew Chem Int 47:6114–6127

23. Salavagione HJ, Miras MC, Barbero CA (2006) Macromol Rapid Commun 27:26–30

24. Salavagione HJ, Martinez G (2011) Macromolecules 44:2685–2692

25. Garbassi F, Morra M, Occhiello E (1994) Polymer surfaces from physics to technology. Wiley, Chichester

26. Wu S (1982) polymer interfaces and adhesion. Marcel Decker, New York

27. Pawde SM, Deshmukh K (2009) Polym Eng Sci 49:808–818

28. Fowkes FM (1963) J Phys Chem 67:2538–2541

29. Good RJ (1993) In contact angle, wettability and adhesion. In: Mittal KL (ed) VSP Utrecht, The Netherlands

30. Moussa S, Atkinson G, Shall MSE, Shehata A, Abouzeid KM, Mohamed MB (2011) J Mater Chem 21:9608–9619

31. Tikka HK, Suvanto M, Pakkanen TA (2004) J Colloid Interf Sci 273:388–393

32. Gudarzi MM, Sharif F (2012) Exp Polym Lett 6:1017–1031

33. Surajit K, Ankur KG, Swapan KD (2013) J Mater Sci 48:1729–1739

34. Van Oss CJ, Giese RF (2002) Colloids and surface properties of clay and related minerals. Marcel Dekker, New York

35. Deshmukh RR, Shetty AR (2008) J Appl Polym Sci 107:3707–3717

36. Fowkes FM (1962) J Phys Chem 66:382–382

37. Fowkes FM (1968) J Colloid Interf Sci 28:493–505

38. Dann RJ (1970) J Colloid Interf Sci 32:302–320

39. Frank EM (2003) In contact angle, wettability and adhesion. In: Mittal KL (ed) VSP: Utrechtp.219

40. Anastasiadis SH (1998) J Rheol 42:795–812